SPECIAL PROJECT PROGRESS REPORT

Reporting year	2021……………………………………………………
Project Title:	Convective phenomena at high resolution over Europe and the Mediterranean…………………………………
Computer Project Account:	spptsoar……………………………………………….
Principal Investigator(s):	Pedro Matos Soares ……..……………………………
Affiliation:	Portugal……………………………………….……
Name of ECMWF scientist(s) collaborating to the project (if applicable)	……………………………………………………….…… ……………………………………………………….……
Start date of the project:	2020/01/01………………………………………………..
Expected end date:	2022……………………………………………….……

Computer resources allocated/used for the current year and the previous one

		Previous year		**Current year**	
		Allocated	Used	Allocated	Used
High Performance Computing Facility	(units)	9 500 000	6816410.38	9 500 000	5206705.01
Data storage capacity	(Gbytes)	1000		1000	

Summary of project objectives

The main goal is to study how convective storms and the associated precipitation extremes would evolve with climate change at the end of the century. To do so, the Coupled Model Intercomparison Project-phase 5 EC-EARTH Global model version is downscaled, considering the RCP8.5 scenario and the Weather Research and Forecasting (WRF) was the Regional Climate Model chosen. Two nested domains were used. The first with an approximate 15 km horizontal resolution, covering the same region as EURO-CORDEX, and a second inner domain over the Alps and central Europe, with a 3 km horizontal resolution. The downscaled data covers the period 2089-2099, with the first year as spin-up. We will thus investigate the convective frequency, duration and intensity changes associated to climate change. Moreover land-atmosphere interactions will also be explored.

Summary of plans for the continuation of the project

In what concerns the study regarding the response of the surface climate to different model options, the future plans consist in the analysis of the impact of different runoff and groundwater options in soil moisture, surface runoff and drainage. Also, the land water balance will be investigated to complement the land energy balance results. In this sense, the analysis of the soil moisture–temperature and soil moisture–precipitation interactions will be explored. Moreover, new simulations with land use changes will be performed (Davin et al 2020).

Regarding the convective scale simulations, a characterization of mid latitude storms, together with an assessment on land-atmosphere interactions related to convective phenomena will be performed. To this end a new simulation covering an historical period is required.

Summary of results

1) Transition from wet and dry regimes: WRF sensitivity to surface model options

Four simulations with the WRF model were carried out with different land surface model schemes for the 2004-2006 period, driven by ERA5 reanalysis. The WRF model version 4.2 was used for the simulations over the European domain with a horizontal resolution of 12 Km and 50 vertical levels, which follows the CORDEX guidelines (Giorgi et al. 2009). The following physical parameterisations are used in the WRF setup for the four simulations (Table 1): the rapid radiative transfer model for global circulation models scheme for longwave and shortwave radiation; the planetary boundary layer Yonsei University scheme; the Grell-Freitas (GF) cumulus scheme; the GRIMS (Global/Regional Integrated Modelling System) shallow convection scheme; the microphysics Thompson aerosol-aware scheme; and the revised MM5 surface layer scheme. For the first experiment, the Noah land surface model was used. For the remaining simulations, the Noah-MP (multi-physics) land surface model was used with different runoff and groundwater options: (1) original surface and subsurface runoff (free drainage), (2) TOPMODEL with groundwater and (3) Miguez-Macho & Fan groundwater scheme. The other Noah-MP options used are described in Table 2.

Table 1. A list of the four simulations containing the physic parameterization options.

Schemes \ Experiment	WRF_NOAH	WRF_NOAH-MP_1	WRF_NOAH-MP_2	WRF_NOAH-MP_3
Radiation	RRTMG			
PBL	YSU			
Cumulus	Grell-Freitas			
Shallow convection	GRIMS			
Microphysics	Thompson 28			
Surface layer	Revised MM5			
LSM	NOAH	NOAH-MP	NOAH-MP	NOAH-MP

Table 2. NOAH-MP LSM configuration used in three simulations.

	Options \ Experiment	WRF_NOAH-MP_1	WRF_NOAH-MP_2	WRF_NOAH-MP_3
NOAH-MP Options	Dynamic vegetation	Off; use input LAI; calculate FVEG		
	Runoff and groundwater	Original surface and subsurface runoff (free drainage)	TOPMODEL with groundwater	Miguez-Macho & Fan groundwater scheme
	Stomatal resistance	Ball-Berry		
	Surface layer drag coefficient	Monin-Obukhov		
	Soil moisture factor for stomatal resistance	CLM		
	Supercooled liquid water	No iteration		
	Soil permeability	Koren's iteration		
	Radiative transfer	Two-stream applied to vegetation fraction		
	Ground surface albedo	CLASS		
	Precipitation partitioning between snow and rain	Snow when SFCTMP<TFRZ		
	Soil temperature boundary condition	TBOT at 8m from input file		
	Snow/soil temperature time	Semi-implicit		
	Glacier treatment	Includes phase change		
	Surface evaporation resistence	Sakaguchi and Zeng 2009		
	Defining soil properties	Use input dominant soil texture		
	Crop model	No crop model, will run default dynamic vegetation		

The first step of this work was to perform an extensive evaluation of all simulations against observations. This is an important step to determine the quality of the simulations. In this way, precipitation, maximum and minimum temperatures from all simulations were compared against observations. The new version of the Europe-wide E-OBS temperature and precipitation data set is used to compare with the output of the simulations performed. This dataset has a regular grid with 0.1^{o} spatial resolution.

For each grid point and time scales [daily, monthly, seasonal, and yearly], the following standard statistics will be computed: bias, normalized bias, mean absolute error, mean absolute percentage error, root mean square error, standard deviation for the RCMs and evaluation data, normalized standard deviation, spatial correlation, and the Willmott – D Score. Additionally, the probability density Function matching scores will be also computed, as well as the Yule-Kendall skewness measure.

Figure 1 (a and b) displays two standard statistical errors (bias% and MAPE for precipitation; bias and MAE for maximum and minimum temperatures) focused on the four simulations' ability to represent the mean precipitation (P), maximum (Tx) and minimum (Tn) temperatures at different temporal scales, from daily, monthly, seasonally to yearly. Looking at precipitation relative bias, one may conclude that all simulations performed overestimate this field. MAPEs indicate a high difference between daily and the remaining time scales. The large values of both the S and the S90 scores above 80%, means that over 80% of the model PDFs matches the observations. In the case of S90, giving the same weight to the PDF under and above the 90th percentile, these high values also appear. In what regards the maximum and minimum temperatures, all simulations show a cold bias. Except the Tx from Noah-MP3, the remaining simulations have an absolute bias less than 2 ^{o}C. Looking to the MAEs, most of the values are similar to the absolute bias. This similitude between the absolute bias value and MAE also points to a systematic negative bias which could be due to a possible negative cold bias in the atmospheric forcing. This issue needs to be investigated through additionally analysis, like a regional evaluation.

Taking the first simulation (Noah) as reference, a seasonal comparison between all simulations were carried out for precipitation, mean skin temperature and 2-m temperature. Figure 2 displays seasonal precipitation from WRF with Noah scheme and its difference from WRF with Noah-MP schemes. For DJF (winter season), the Noah-MP simulations underestimate precipitation in most of the domain. In specific regions, like Iberian Peninsula and France, an overestimation is observed. Results for JJA (summer season) present higher differences. Noah-MP3 shows an overestimation of precipitation,

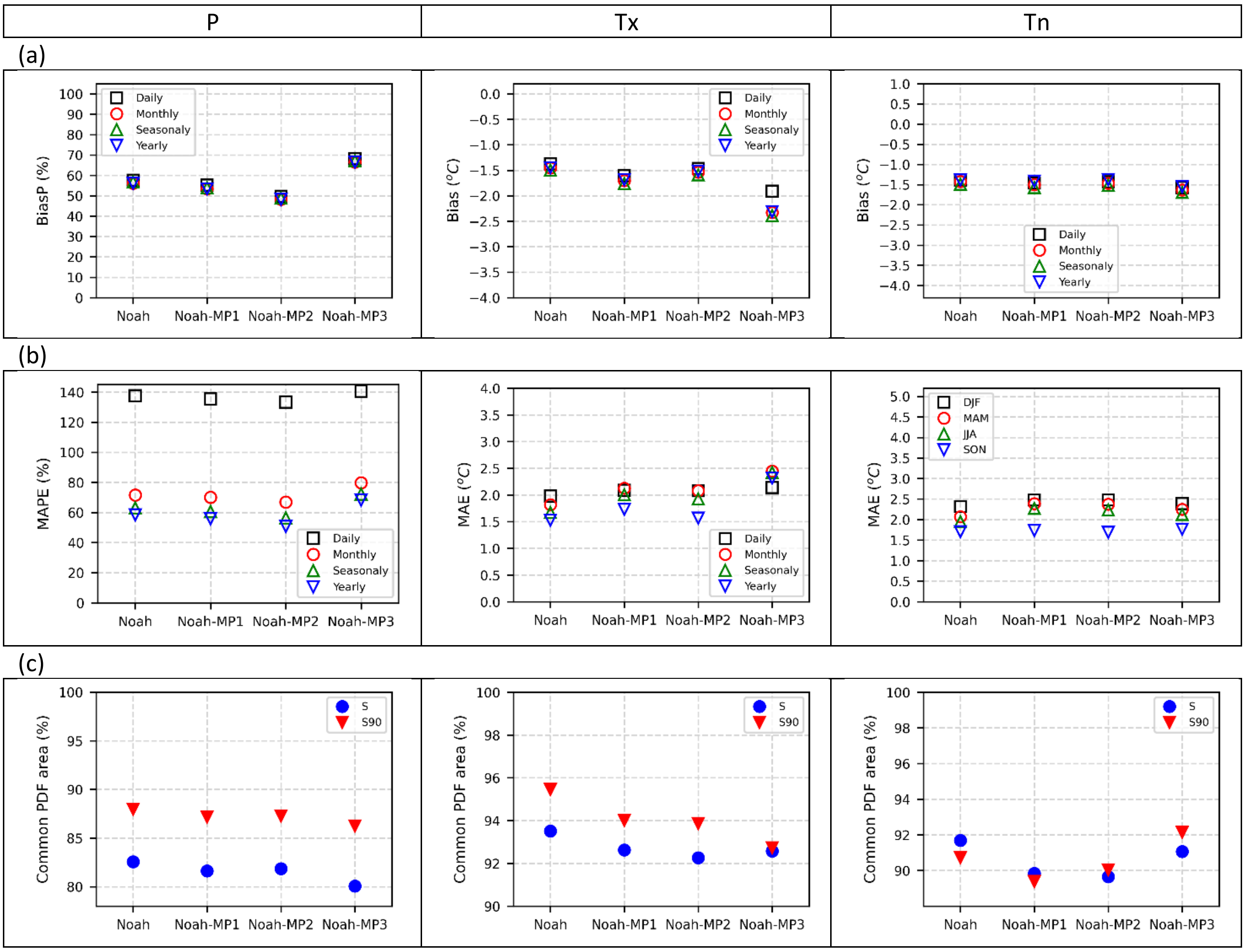

Figure 1. Error measures of simulations precipitation (left), maximum (middle) and minimum (right) temperature for the European domain (2004-2006). The bias is represented in (a), and MAE is represented in (b). For precipitation, both metrics were normalized by the mean, and the values are given in percentage. The errors are computed for different time periods (daily in black, monthly in red, seasonally in green and yearly in blue) pooling all data together. (c) PDF matching skill scores S (blue) and S90 (red) for daily precipitation (left), maximum (middle) and minimum (right) temperature, respectively, PDFs simulated by the test simulations over European domain during the 2004-2006 period.

with values higher than 100 mm in north of Iberian Peninsula, France, and southern part of Eastern Europe. In the northern part of Eastern Europe, an underestimation is observed. Figures 3 and 4 are similar to Figure 2 but for mean skin temperature and 2-m mean temperature, respectively. The results between these two variables are similar. A negative bias is observed in DJF in all simulations, being larger in Eastern Europe, where the differences can reach -3 °C. For summer, Noah-MP1 and Noah-MP2 present a warm bias, which is more noticeable in skin temperature for Mediterranean regions. Noah-MP3 shows a cold bias in the whole domain, except in the northern part of Eastern Europe. Like the other simulations, the negative bias is more pronounced in skin temperature.

The analysis of the land energy balance is in development to address the soil moisture and temperature interactions.

2) Convection

For the assessment on convective phenomena, the WRF model version 3.8.1, with 50 vertical levels was used. Two domains are considered: EURO-CORDEX at a 15 km resolution (EUR) and an inner domain over the Alps region with a very high-resolution of 3 km (ALP). This simulation is included within the Flagship Pilot Study on Convection and covers the future period from 2089-2099, with the first year as spin-up. The Historical counterpart of this simulation will also be assessed, thus a climate

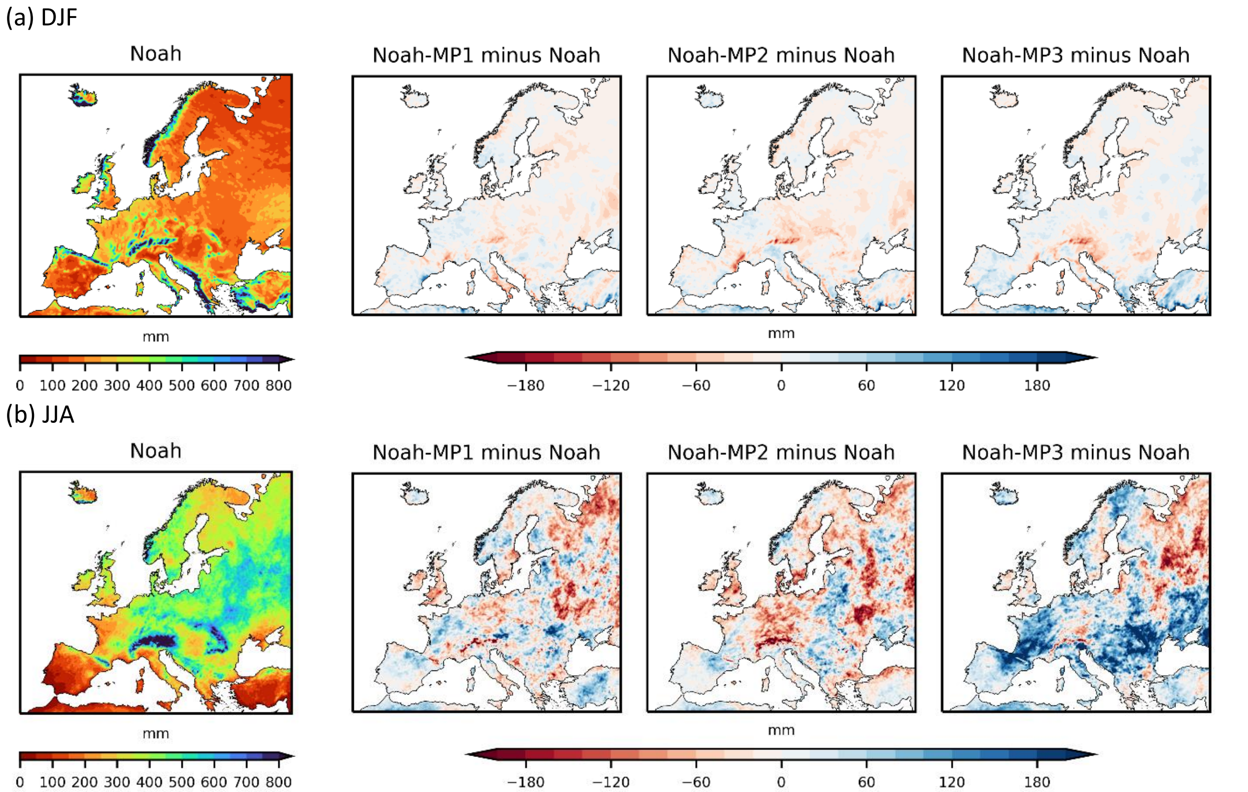

Figure 2. Seasonal (DJF and JJA) precipitation from WRF with Noah scheme and its difference from WRF runs with Noah-MP schemes.

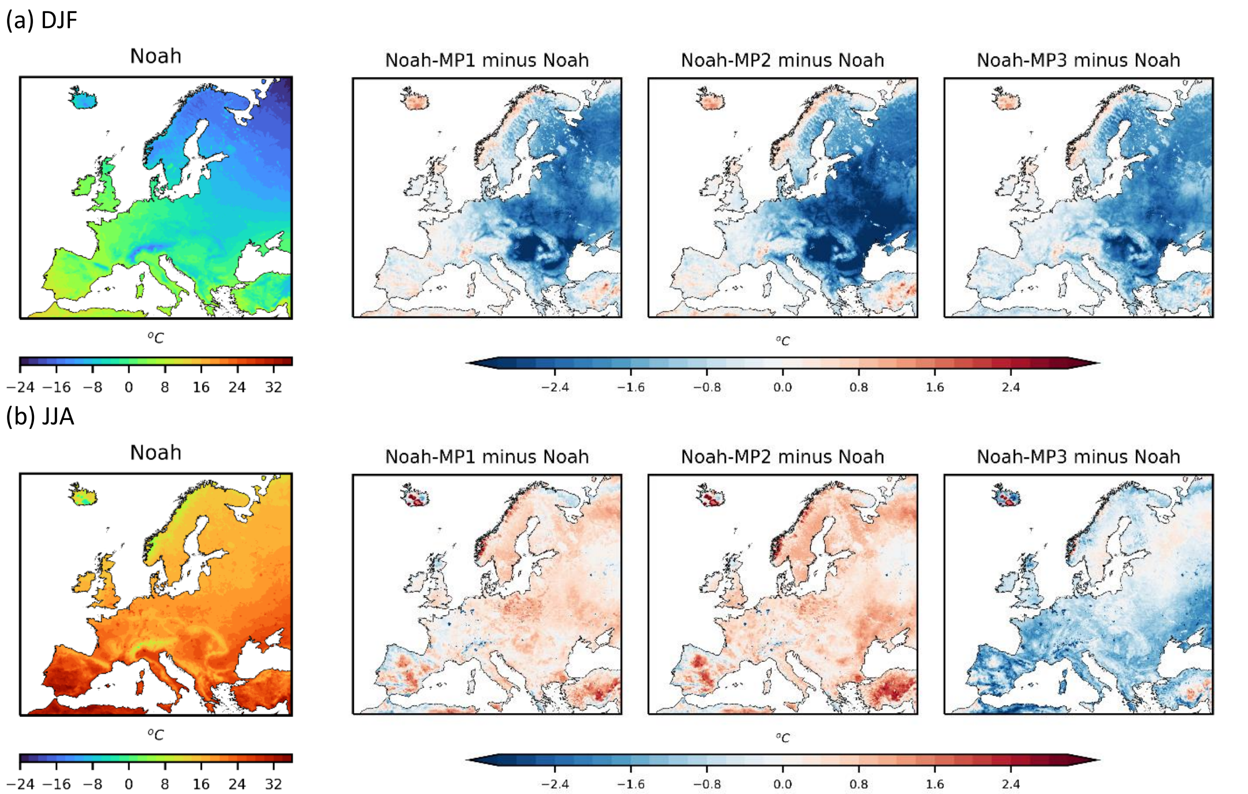

Figure 3. Seasonal (DJF and JJA) skin temperature from WRF with Noah scheme and its difference from WRF runs with Noah-MP schemes.

change on convective activity and land-atmosphere coupling will be performed. The results shown here are preliminary and only considers this simulation. Figure 5a shows the mean precipitation cycle for the EUR domain. Throughout the year most precipitation occurs over the sea, particularly

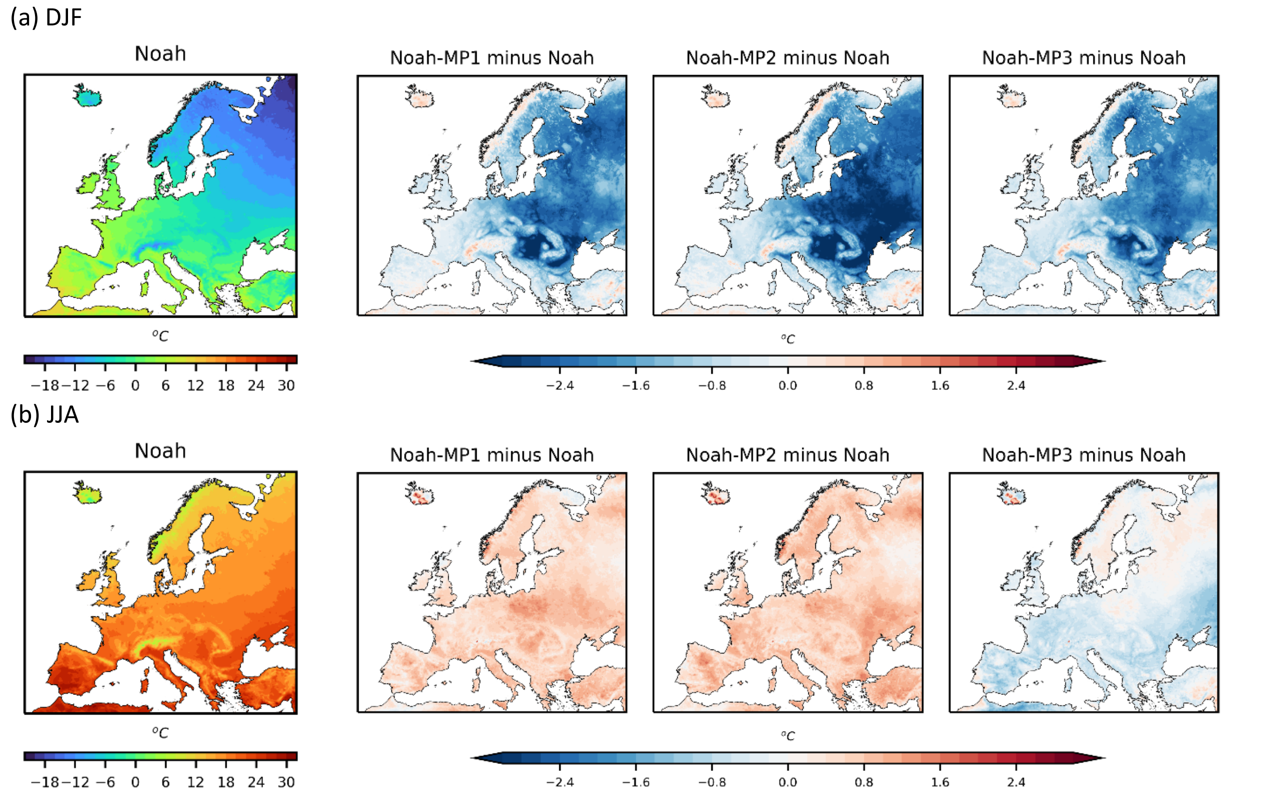

Figure 4. Seasonal (DJF and JJA) 2-m mean temperature from WRF with Noah scheme and its difference from WRF runs with Noah-MP schemes.

over the North Sea, Norwegian sea and at the north of the Iberian Peninsula, with a clear land-sea contrast. Still areas around the Mediterranean Sea, such as Italy or Greece reveal high precipitation values from October to June. Figure 5b displays the 95th percentile for each month. As expected from the previous panel (Figure 5a), most extreme precipitation occurs over the nonwestern part of the EUR domain. However, for October, November and December, the Mediterranean regions, more specifically over Italy, Alps and Greece also reveal higher values. Moreover, during winter, the northwestern region of the Iberian Peninsula also displays significant values.

In Figure 6, similar to figure 5, the precipitation cycle is shown, but for the ALP domain. Figure 6a reveals the monthly cycle, where most precipitation occurs primarily from October to March with, as expected, higher values over the Alps. During the other months, in particularly from June to September, precipitation is more focused over the Alps. Overall, the values for the late spring and summer months are lower. Figure 6b displays the 95th percentile for each month of the year, thus returning an estimate of the extreme precipitation. The influence of the Alpine mountains is evident for all months, with values reaching and surpassing the 25 $mm\ day^{-1}$.

The difference for precipitation with both resolutions (15 km and 3 km) is evident over the Alps mountain range, particularly for extreme precipitation. In the last case, the finer details allow more extreme values for this variable, thus consisting in added value due to the use of a kilometer-scale simulation.

References:

Giorgi, F., Jones, C. and Asrar, G.R., 2009. Addressing climate information needs at the regional level: the CORDEX framework. World Meteorological Organization (WMO) Bulletin, 58(3), p.175.

Davin, E.L., Rechid, D., Breil, M., Cardoso, R.M., Coppola, E., Hoffmann, P., Jach, L.L., Katragkou, E., Noblet-Ducoudré, N.D., Radtke, K. and Raffa, M., 2020. Biogeophysical impacts of forestation in Europe: first results from the LUCAS (Land Use and Climate Across Scales) regional climate model intercomparison. Earth System Dynamics, 11(1), pp.183-200.

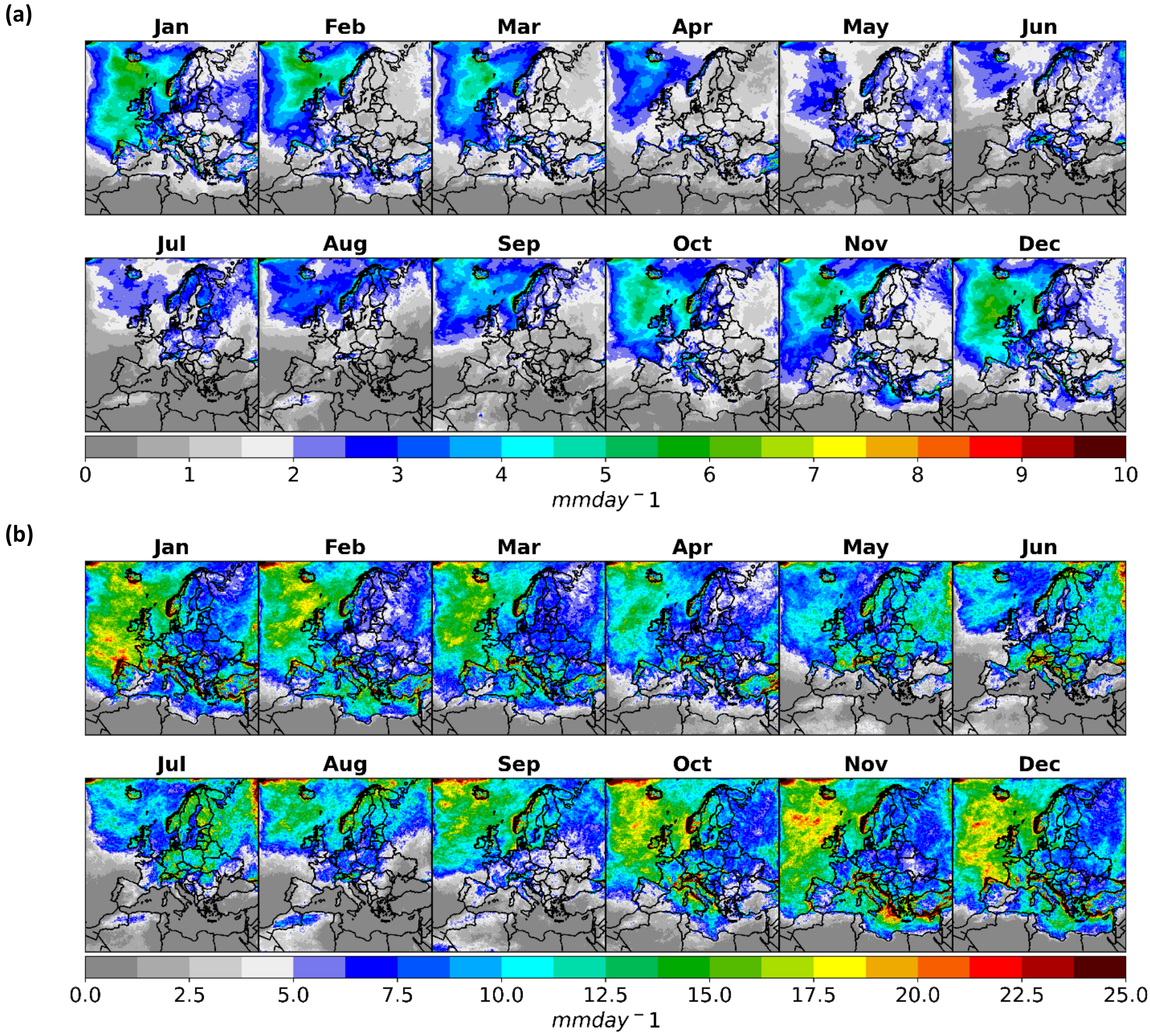

Figure 5. (a) Mean daily precipitation and (b) the 95th percentile for each month of the year, considering the period from 2090-2099. The results are for the outer nest at approximately 15 Km horizontal resolution covering the EURO-CORDEX domain, for the RCP 8.5 scenario.

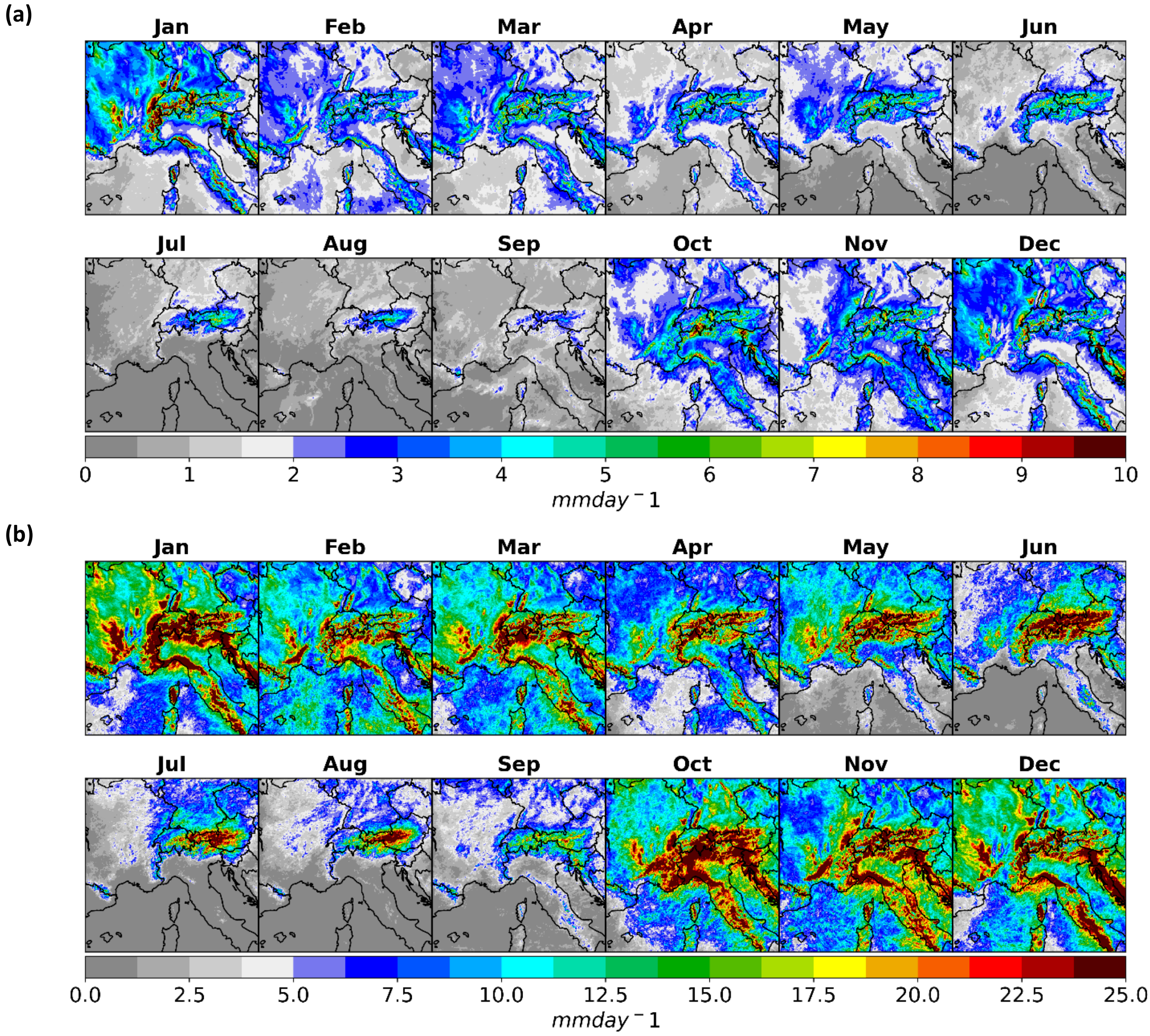

Figure 6. (a) Mean daily precipitation and (b) the 95th percentile for each month of the year, considering the period from 2090-2099. The results are for the inner nest at approximately 3 Km horizontal resolution covering the ALP domain, for the RCP 8.5 scenario.